ACS APPLIED MATERIALS & INTERFACES

Applications of Polymer, Composite, and Coating Materials

Thiol-Yne Click Post-Modification for the Synthesis of Chiral Microporous Organic Networks for Chiral Gas Chromatography

Yuanyuan Cui, Cheng-Xiong Yang, and Xiu-Ping Yan

ACS Appl. Mater. Interfaces, **Just Accepted Manuscript** • DOI: 10.1021/acsami.9b22023 • Publication Date (Web): 02 Jan 2020

Just Accepted

is published by the American Chemical Society. 1155 Sixteenth Street N.W., Washington, DC 20036

Thiol-Yne Click Post-Modification for the Synthesis of Chiral Microporous Organic Networks for Chiral Gas Chromatography

Yuan-Yuan Cui†, Cheng-Xiong Yang*,† and Xiu-Ping Yan‡

† College of Chemistry, Research Center for Analytical Sciences, Tianjin Key Laboratory of Biosensing and Molecular Recognition, Nankai University, Tianjin 300071, China

‡ State Key Laboratory of Food Science and Technology, International Joint Laboratory on Food Safety, Institute of Analytical Food Safety, School of Food Science and Technology, Jiangnan University, Wuxi 214122, China

ABSTRACT: Microporous organic networks (MONs) have shown great potential in diverse domains recently. However, the application of MONs in chiral separation or catalysis has been largely lagged due to the lack of chiral MONs and the challenge to synthesize chiral MONs. Here we report a facile thiol-yne click strategy to post-synthesize chiral MONs for the first application in chiral gas chromatography. Three chiral MONs with different chiral centers were rationally designed and synthesized to fabricate their capillary columns for gas chromatographic resolution of various chiral compounds with better resolution than three commercial chiral capillary columns. These results show the great potential of the thiol-yne click strategy for constructing newly chiral MONs and their application in chiral separation.

KEYWORDS: thiol-yne click strategy, microporous organic networks, post-modification, chiral separation, gas chromatography

1. INTRODUCTION

Chiral separation still remains an extremely significant and challenging topic in chemistry, pharmaceutical industry, biology and material science as enantiomers may possess completely different biological and pharmacology activity in most cases.[1,2] Nonetheless, chiral separation faces great difficulty due to the identical physical and chemical behavior of two individual enantiomers.[3] Traditional methods in chiral separation include chemical, enzyme/biological and chromatographic separation.[1] Chromatography based on chiral stationary phase (CSP) is regarded as a highly selective and efficient method in chiral separation.[3] Recently, advanced functional materials like metal-organic frameworks (MOFs), covalent-organic frameworks (COFs), porous organic cages (POCs) and metal-organic cages (MOCs) have been engineered as newly CSPs in chiral chromatographic resolution of diverse enantiomers.[4-10] Rational design and synthesis of novel and efficient chiral porous materials in chiral chromatography are of urgent desirable either in the evolution of chiral chromatography or in the development of material science.

Microporous organic networks (MONs) are a recent class of amorphous and functional materials via cross coupling reaction of rigid organic building blocks.[11,12] Given their good chemical and thermal stability, large surface area and tunable porosity with functionalized internal networks, MONs have shown great potential in various applications such as catalysis, sensing, adsorption, lithium ion batteries, drug delivery and nanofiltration.[13-25] Compare with the MOFs, the MONs show better chemical stability and easier structural modification and designing. The MONs also own easier synthesis and much convenient engineering on other matrix than COFs. By contrast, the much ordered and regular structures of MOFs and COFs than MONs usually lead to the construction of highly crystalline porous materials of MOFs and COFs. However, the synthesis and application of chiral MONs is still at a very early stage due to limited chiral MONs available and their challenging synthesis. Chiral MONs can be prepared either directly[26-28] or via post-modification.[29] Chiral MONs using chiral BINAP, TADDOL and BINOL monomers have been reported via direct synthesis approach.[26-28] However, multistep and complex derivatizations are needed to synthesize these chiral monomers, thus, impeding their further applications.

Post-synthetic modification (PSM) has been regarded as a feasible way to construct functional materials because of its convenient and economic synthesis and the available of diverse molecules and functional groups.[3] The abundant functionalized groups (e.g. amino, carboxyl, alkyne) on the networks of MONs make PSM quite convenient. For example, Cooper's group reported the synthesis of achiral anhydride modified MONs via the PSM of amino groups on MONs.[29]

Thiol-yne click reaction is one of the most significant synthetic techniques in chemistry due to its simplicity, efficiency, and functionality tolerance.[30] The enriched internal and terminal alkyne groups on MONs are also capable for PSM through thiol-yne click reaction. In 2012, Weber's group reported the first example of thiol-yne click strategy to synthesize aliphatic alcohols functionalized MONs.[31] After that, PSM of MONs via thiol-yne click reaction has been investigated for drug delivery, $PM_{2.5}$ capture, light-driven hydrogen evolution, uranium and Cr (VI) removal.[24, 32-35] Although great efforts have been made for PSM synthesis of achiral MONs, the synthesis of chiral MONs via thiol-yne click protocol has been largely lagged. Although chiral BINOL-based MONs as novel chiral fluorescence sensor for amino alcohols has been reported,[27] the

application of chiral MONs in chiral separation is still an unexplored area and not to mention how to regulate the selectivity of chiral MONs.

Herein, we report a facile thiol-yne click strategy to post-synthesize chiral MONs for chiral gas chromatography (GC). Chiral thiol-based molecules 1-thloglycerol (TGC), mercaptosuccinic acid (MSA) and N-acetylcysteine (NAC) were reasonably decorated on the networks of the MONs via the thiol-yne click post-modification with high grafting efficiency and universality. Three chiral MONs with individual chiral centers or recognition sites were rationally designed and synthesized to fabricate their coated capillary columns for GC separation of diverse chiral compounds. The prepared chiral MONs coated capillary columns offered high resolution for various enantiomers with better resolution and selectivity than three commercial capillary columns. The developed thiol-yne click strategy opens a promising way for the design and construction of chiral MONs in chiral separation.

2. EXPERIMENTAL SECTION

2.1. Chemicals and Materials. 1,3,5-Triethynylbenzene (98%, Tongchuangyuan, China) was used as the monomer. The copper(I) iodide (99.99%), 1,4-dibromobenzene

(98%), bis(triphenylphosphine)palladium dichloride (> 98%), mercaptosuccinic acid (MSA, 98%), 1-thloglycerol (TGC, 95%), N-acetylcysteine (NAC, 99%) and 2,2'-azobis(2-methylpropionitrile) (AIBN, 99%) were obtained from Aladdin Chemistry Co., Ltd. (Shanghai, China). HCl and NaOH were supplied by Guangfu Co., Ltd. (Tianjin, China). *N,N*-dimethylformamide (DMF, Superdry) was bought from J&K Co., Ltd. (Beijing, China). Ultrapure water was supplied by Wahaha Co., Ltd. (Tianjin, China). Triethylamine, chloroform, methanol, ethanol, tetrahydrofuran (THF) and acetone were obtained from Concord Co., Ltd. (Tianjin, China).

2.2. Synthesis of MON and Chiral MONs. The MON was synthesized according to Jiang *et al.*[36] Briefly, 1,3,5-triethynylbenzene (300.0 mg, 2.0 mmol), 1,4-diiodobenzene (660.0 mg, 2.0 mmol), bis(triphenylphosphine)palladium dichloride (50.0 mg, 0.07 mmol) and CuI (15.0 mg, 0.08 mmol) were placed in a three-necked flask. The mixture was degassed and refilled with nitrogen three times. The DMF (40.0 mL) and triethylamine (40.0 mL) were then injected into the flask. The mixture was heated to 90 ^{o}C for 24 h under magnetic stirring. After cooling to room temperature, the dark brown powder was collected by centrifugation (10000 rpm, 5 min) and washed with chloroform,

methanol and acetone, respectively. The crude product was further purified with hot methanol by Soxhlet extraction for 72 h and then dried under vacuum at 70 °C for 24 h to give a light brown product.

The MON-TGC was synthesized according to Han *et al* with minor modifications.[34] MON (80 mg), TGC (1620 mg) and AIBN (82 mg) were dissolved with 15.0 mL of anhydrous DMF. The mixture was stirred at 90 °C for 24 h under nitrogen protection. The product was gathered by centrifugation (10000 rpm, 5 min) and treated with hot THF and acetone three times, and then dried under vacuum at room temperature overnight. Similarly, MON-MSA and MON-NAC were prepared according to above method via altering the TGC (1620 mg) to MSA (2250 mg) and NAC (2430 mg), respectively.

2.3. Preparation of Chiral MONs' Coated Capillary Columns. The bare fused silica capillary (0.25 mm i.d. × 30 m long, Yongnian Optic Fiber Plant, China) was pretreated via the previously reported steps before the dynamic coating of chiral MONs' capillary columns.[3] The chiral MON-TGC coated capillary column was fabricated via a dynamic coating method. One milliliter ethanol suspension of MON-TGC (2 mg mL^{-1}) was firstly

injected into the above pretreated capillary column under N_2 flow, and then pushed forward in the capillary column at a N_2 flow rate of 0.2 mL min^{-1} to yield a thin layer on the inner surface of the capillary column. After coating, the capillary column was conditioned under N_2 flow through the temperature program of 30 °C to 250 °C at a rate of 2 °C min^{-1}, and 250 °C for 120 min. The chiral MON-MSA and MON-NAC coated capillary columns were prepared using the same method to that for MON-TGC coated capillary column.

3. RESULTS AND DISCUSSION

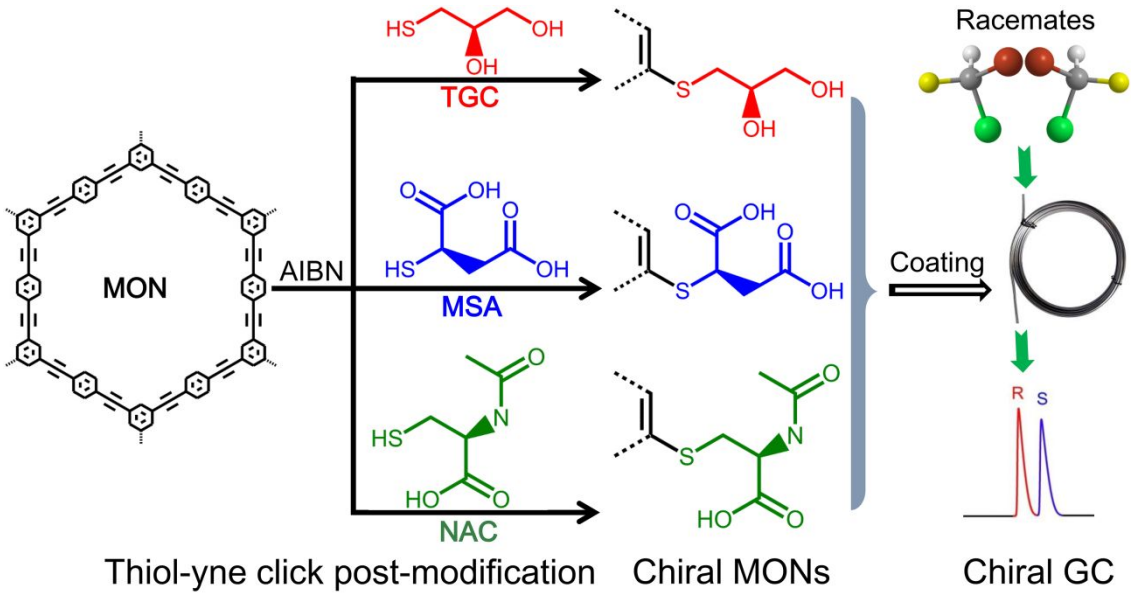

Scheme 1. Illustration for the thiol-yne click strategy to post-synthesize chiral MONs for chiral GC.

3.1. Synthesis and Characterization of MON and Chiral MONs. A 2D MON prepared via the Sonogashira coupling of 1,4-diiodobenzene and 1,3,5-triethynylbenzene was selected as the pristine MON for thiol-yne click PSM.[36] The selected 2D MON possesses large surface area, enriched ethynyl groups, good thermal and chemical stability, which are all of great benefit for PSM via thiol-yne click reaction. In addition to these above advantages, the large accessible open cavities of the MON provide great opportunity for the designed chiral thiol molecules to enter for effective thiol-yne click reaction with the ethynyl groups on MON's inner surface.[36]

The bottleneck of chiral chromatography is the rational design and synthesis of highly efficient CSPs. The chiral groups or recognition sites on CSPs played key roles during chiral separation.[3] The chiral microenvironment, π-π, hydrogen bonding and van der Waals interactions are the essential separation mechanisms in chiral chromatography. Incorporation of chiral molecules with proper chiral groups or different chiral recognition sites and dimension in MONs not only offers the chiral functions and microenvironment, but also provides different chiral selectivity for the evolution and development of chiral MONs in chiral separation and recognition.

To tune the selectivity of chiral MONs and to elucidate the separation mechanisms of chiral MONs, thiol molecules TGC, MSA and NAC with different chiral groups and molecular dimension were selected to post-synthesize chiral MONs via the thiol-yne click reactions (Scheme 1). Although all these three thiol molecules offer possibility for hydrogen-bonding interaction to racemates during the chiral separation process, their hydrogen-bonding receptors or donors are quite different (-OH for TGC, -COOH for MSA, and N-acetyl and -COOH for NAC, respectively). In addition, the chiral microenvironment of these three chiral MONs may differ due to their different molecular dimensions. All these minor differences would lead to different chiral selectivity during chiral separation.

The synthesized chiral MON-TGC, MON-MSA and MON-NAC were characterized by solid ^{13}C nuclear magnetic resonance (^{13}C NMR) spectroscopy, transmission electron microscopy (TEM), N_2 adsorption-desorption experiments, scanning electron microscopy (SEM), Fourier transform infrared spectroscopy (FT-IR), X-ray diffraction (XRD), thermogravimetric analysis (TGA), circular dichroism spectra (CD), water contact angle measurements and X-ray photoelectron spectroscopy (XPS), (Figures 1-2

and Figure S1). The FT-IR adsorption at 830 and 1585 cm^{-1} correspond to the vibrational stretching of C-H and C-C in pristine MON's aromatic rings.[37] The characteristic peak at 2200 cm^{-1} for C≡C reveals the presence of alkynyl groups on MON. The appearance of characteristic peaks at 3420 cm^{-1} (-OH) and 1038 cm^{-1} (C-O) for TGC, 1716 cm^{-1} (C=O) and 3450 cm^{-1} (-OH) for MSA, and 1726 cm^{-1} (C=O on -COOH) and 1662 cm^{-1} (C=O on -NH-C=O) for NAC on FT-IR spectra of MON-TGC, MON-MSA and MON-NAC demonstrates the successful synthesis of the designed chiral MONs (Figure 1a). In addition, the disappearance of the characteristic peak of C≡C at 2200 cm^{-1} for the pristine MON along with the S-H vibration peak at 2555 cm^{-1} for the three chiral MONs confirms the successful addition of thiol molecules onto alkynyl groups via thiol-yne click reaction (Figure 1a).

The appearance of XPS peaks of S2s and S2p for MON-TGC and MON-MSA, and N1s, S2s and S2p for MON-NAC also indicated the successful PSM of chiral MONs (Figure 1b). The grafting contents of TGC, MSA and NAC on chiral MONs were then calculated according to the XPS results. As expected, the S element was not detected in the pristine MON. Based on the content of S, the modified TGC, MSA and NAC in

their individual chiral MONs were determined to be 0.61, 0.54 and 0.68 mmol g^{-1}, respectively (Table S1). The N content in MON-NAC was 1.96 wt%, giving the NAC modification content on MON-NAC of 0.70 mmol g^{-1}, comparable to the value calculated from S element (Table S1). TGA analysis showed that the MON and three chiral MONs were all stable up to 300 ^{o}C, which was favorable for their further application in chiral GC (Figure 1c).

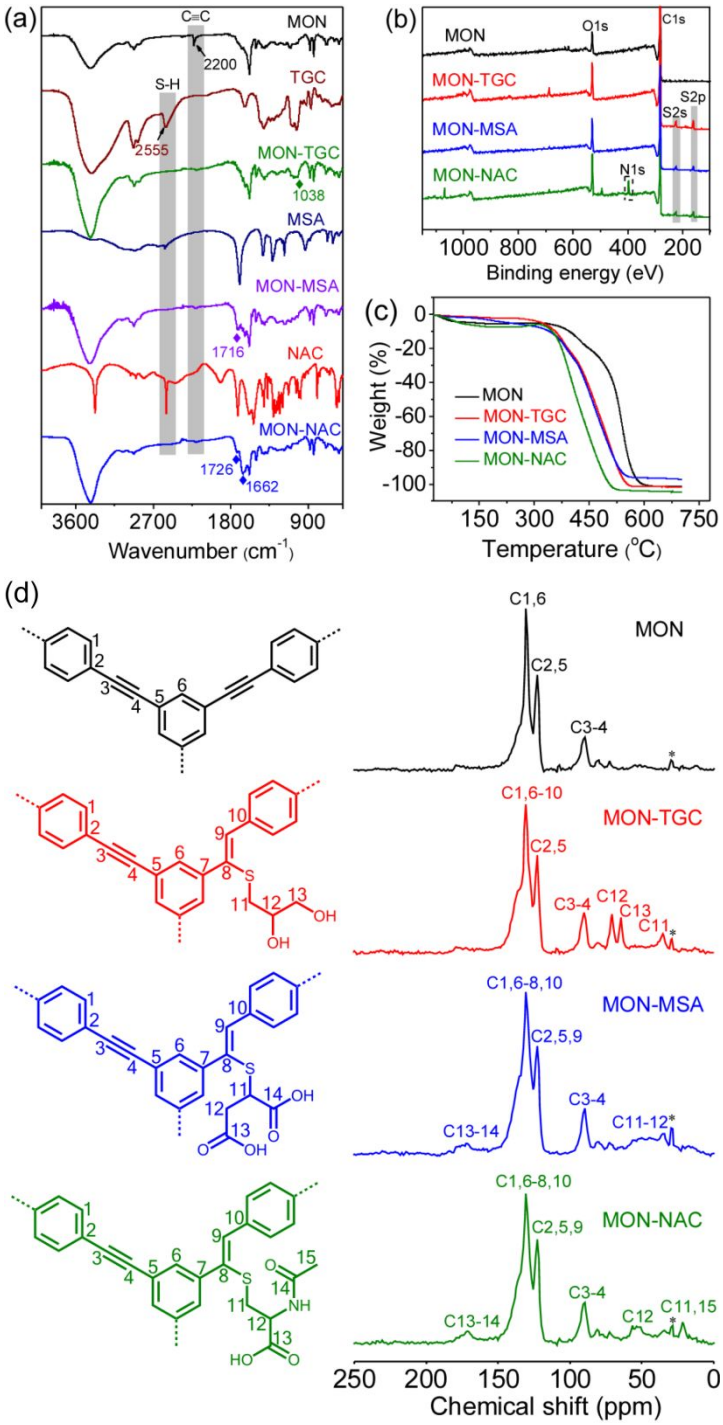
(a)
C≡C
2200
S-H
2555
1038
1716
1726
1662
MON
TGC
MON-TGC
MSA
MON-MSA
NAC
MON-NAC
3600 2700 1800 900
Wavenumber (cm-1)
(b)
MON
MON-TGC
MON-MSA
MON-NAC
O1s
C1s
S2p
S2s
N1s
1000 800 600 400 200
Binding energy (eV)
(c)
Weight (%)
0 -20 -40 -60 -80 -100
MON
MON-TGC
MON-MSA
MON-NAC
150 300 450 600 750
Temperature (°C)
(d)
C1,6
C2,5
C3-4
C1,6-10
C12
C13
C11
C1,6-8,10
C2,5,9
C13-14
C11-12
C11,15
250 200 150 100 50 0
Chemical shift (ppm)

Figure 1. (a) FT-IR spectra of the MON, TGC, MON-TGC, MSA, MON-MSA, NAC, and MON-NAC. (b) XPS wide-scan spectra, (c) TGA curves and (d) solid state ^{13}C NMR spectra of the MON, MON-TGC, MON-MSA, and MON-NAC. Asterisks denote the spinning sidebands.

The solid state ^{13}C NMR peaks at 90-95 and 120-150 ppm were ascribed to the alkynes and aromatic rings for the pristine MON (Figure 1d).[12,19] These peaks still retain on the chiral MONs, indicating the original networks of the MON were kept during the thiol-yne click PSM process. In addition, there are a few new peaks in solid ^{13}C NMR spectra, depending on their original chiral molecules (Figure 1d). For MON-TGC, the peaks of aliphatic carbon connected to hydroxyl groups appear at 60-70 ppm, corresponding to the C12 and C13. The peak at 35 ppm is assigned to aliphatic carbon of C11. For MON-MSA, the peaks of carbonyl groups and aliphatic carbon at 170 and 40 ppm are ascribed to the C13-14 and C11-12 carbons, respectively. Similarly, three new peaks at 178, 60 and 30 ppm on MON-NAC are assigned to C13-14, C12, and C11 and C15, respectively. These results further show the selected chiral molecules were successfully incorporated onto chiral MONs' networks.

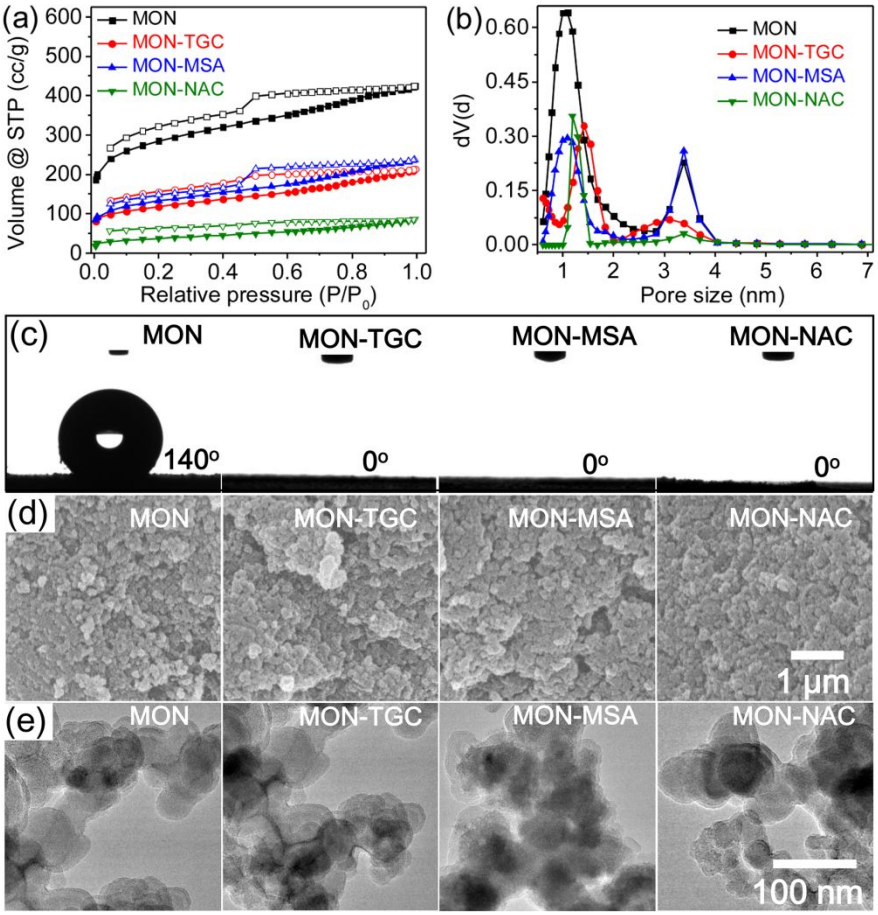

Figure 2. (a) N_2 adsorption-desorption isotherms, (b) pore size distribution, (c) water contact angles, (d) SEM images, and (e) TEM images of the MON, MON-TGC, MON-MSA, and MON-NAC. The scale bars of MON, MON-TGC, MON-MSA are the same as those for MON-NAC.

The Brunauer-Emmett-Teller (BET) surface area of the pristine MON was 1032.1 $m^2\ g^{-1}$, while the BET surface areas of MON-TGC, MON-MSA and MON-NAC were reduced to 420.0, 473.1, and 131.1 $m^2\ g^{-1}$, respectively (Figure 2a and Table S2). The pore volume of the chiral MONs was also decreased from 0.68 $cm^3\ g^{-1}$ for the pristine

MON to 0.35, 0.34 and 0.12 cm^3 g^{-1} for MON-TGC, MON-MSA and MON-NAC, respectively (Table S2). The decrease of BET surface area and pore volume for MON-TGC, MON-MSA and MON-NAC are ascribed to the filling of the introduced chiral molecules in the pore of the pristine MON. The differences of pore size distribution of three chiral MONs also resulted from the different chiral molecules modified (Figure 2b). The XRD patterns show the amorphous characteristic of chiral MONs after PSM via thiol-yne click reaction (Figure S1b).

The water contact angle of the pristine MON was 140°, showing its good hydrophobicity. However, the water contact angle drastically decreased to about 0° after the modification of chiral molecules, revealing the successful PSM of chiral molecules and the introduction of chiral molecules led to a great enhancement of hydrophilicity (Figure 2c). The CD spectra of MON-TGC, MON-MSA and MON-NAC exhibit the classic single peaks, indicating the homochirality of three synthesized chiral MONs (Figure S1a). The SEM and TEM images show the amorphous morphology of the MON and three chiral MONs (Figure 2d-e). In addition, the morphology and particle size of the pristine MON did not significantly change after PSM via thiol-yne click strategy (Figure

2d-e). Three capillary columns based on the above chiral MONs were fabricated via the dynamic coating method.[3] The SEM images confirm the successful coating of these chiral MONs on capillary columns (Figure S1c). In addition, the FT-IR spectra and SEM images of these chiral MONs after immersing in ethanol, n-hexane and water for 2 days are also comparable to pristine ones (Figures S2-S3), showing the good stability of these chiral MONs.

3.2. Chiral MONs Coated Capillary Columns for Chiral GC. Diverse racemates were chosen to evaluate the chiral separation performance of these chiral MONs coated capillary columns. The fabricated chiral MONs capillary columns offered high selectivity for chiral alcohols. Eleven chiral alcohols were well separated on these three chiral MONs coated capillary columns (Figure 3 and Table S3-S4). In addition, the chiral selectivities are quite different for these chiral MONs. The difference in enantioselectivity resulted from the difference of chiral recognition sites and steric matching between enantiomers and chiral MONs. The MON-TGC gave good resolution for 2-substitute alcohols with side functional groups. For instance, MON-TGC coated capillary column showed good separation for 4-heptyn-2-ol, 4-pentyn-2-ol,

2-phenyl-4-penten-2-ol, and 5-methyl-2-hexanol enantiomers with alkynyl, alkenyl, benzene or methyl groups (Figure 3a). However, the linear 2-substitute alcohols like 2-pentanol, 2-hexanol, 2-heptanol, 2-octanol and 2-decanol enantiomers without any side chains or substitute functional groups cannot be separated on MON-TGC coated capillary column (Figure S4). In contrast, 3-heptanol enantiomers without any side chains or substitute functional groups were well separated on MON-TGC coated capillary column. Nevertheless, 3-substitute alcohols such as 3-hexanol, 3-octanol, 3-nonanol and 3-decanol enantiomers with shorter or longer alkyl chains than 3-heptanol were not resolved on MON-TGC coated capillary column (Figure S4). These results reveal the steric matching between the chiral MON-TGC's channel and the racemates played significant roles in high resolution GC separation of these chiral alcohols. In addition, the hydrogen bonding interaction (O-H···O) between chiral alcohols and MON-TGC may also play a key role. The retention time's precisions (RSDs, %) of replicate separations of 4-heptyn-2-ol for intra-day, inter-day and column-to-column were in the range of 1.1-7.2%, suggesting the good reproducibility of the prepared MON-TGC columns (Figure S5 and Table S5).

To further show the significant points of chiral microenvironment and steric matching effect in chiral GC and to tune the selectivity of chiral MONs, the MON-NAC with much larger molecular dimension of NAC than TGC was compared (Figure 3b). The racemates of 3-heptanol, 4-methyl-1-heptyn-3-ol and 2-methyl-2,4-pentanediol were baseline separated on MON-NAC coated capillary column (Figure 3b). Compared with the MON-TGC coated capillary column, the chiral separation range of MON-NAC coated capillary column is quite limited, which could be ascribed to the larger molecular dimension of NAC (7.4 $\times$ 7.2 Å) than TGC (5.9 $\times$ 5.2 Å), leading to the decrease of the space for racemates to get in (Figure S6). In addition, the difference of the hydrogen bonding interaction resulted from acetyl and carboxyl groups on MON-NAC and hydroxyl groups on MON-TGC can also realize important roles during the chiral GC.

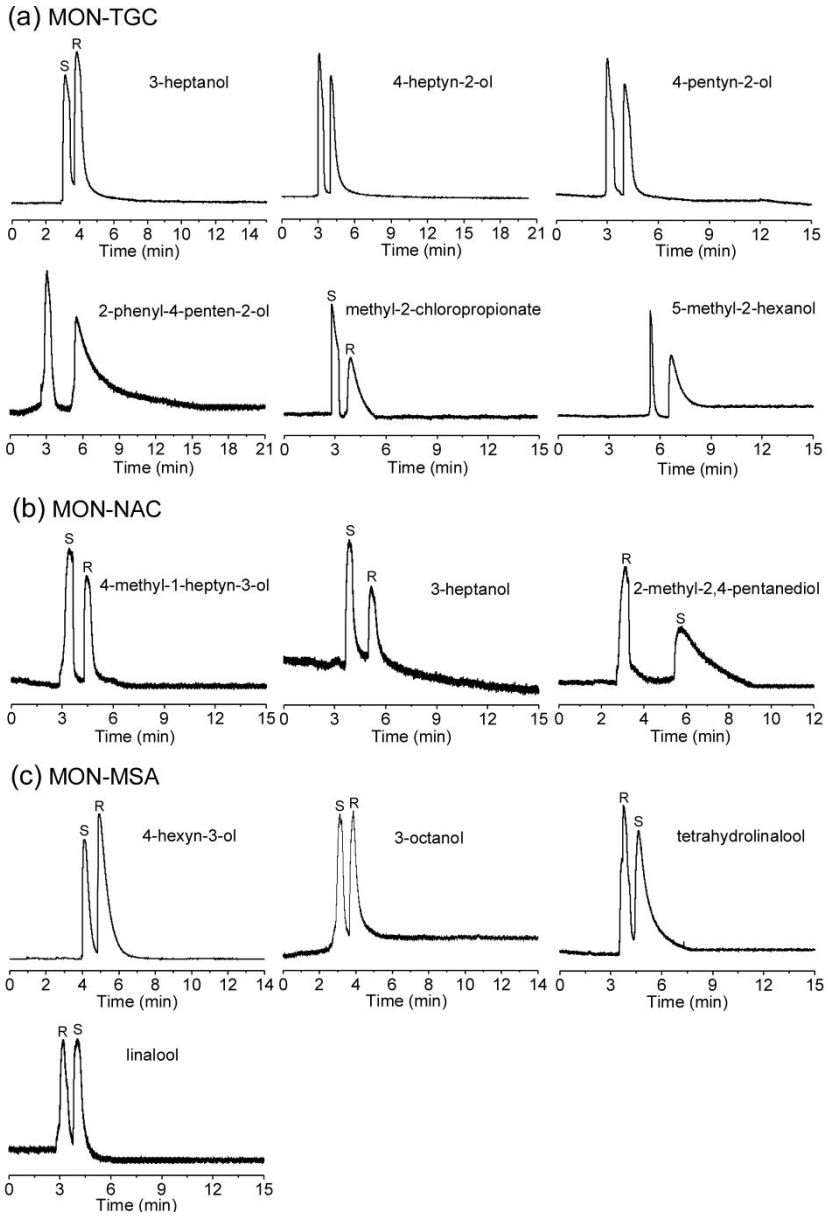

Figure 3. Chromatograms of the chiral MONs coated capillary columns (30 m length × 0.25 mm i.d.) for chiral GC. (a) MON-TGC coated capillary column: 3-heptanol (140 °C), 4-heptyn-2-ol (140 °C), 4-pentyn-2-ol (120 °C), 2-phenyl-4-penten-2-ol (150 °C), methyl-2-chloropropionate (120 °C), 5-methyl-2-hexanol (120 °C). (b) MON-NAC coated capillary column: 4-methyl-1-heptyn-3-ol (110 °C), 3-heptanol (130 °C), 2-methyl-2,4-pentanediol (160 °C). (c) MON-MSA coated capillary column:

4-hexyn-3-ol (100 °C), 3-octanol (160 °C), tetrahydrolinalool (110 °C), linalool (100 °C). All the separations were performed under N_2 flow rate of 2.0 mL min^{-1}.

The MON-MSA coated capillary column offered good selectivity for the enantiomers of alcohols including 3-octanol, 4-hexyn-3-ol, linalool and tetrahydrolinalool (Figure 3c). However, the MON-MSA showed good resolution for 3-substitute alcohols rather than 2- and 4-substitute alcohols (Figure S7). In addition, the linalool derivates were well separated on MON-MSA coated capillary column. More importantly, the prepared three chiral MONs capillary columns all showed high selectivity and resolution for 3-substitute alcohols (3-heptanol and 3-octanol) which were quite difficult to separate and could not be separated either on chiral MOFs, COFs, and POCs coated columns or even on commercial columns.[38] The separation of 3-heptanol and other five racemic alcohols on chiral and non-chiral MONs and three commercialized chiral GC columns were then compared under the same separation conditions (Figure 4, Table 1 and Figure S8). The MON-TGC coated capillary column showed good performance for these analytes under the same separation conditions. These above results all proved the feasibility and highly potential of thiol-yne click strategy to post-synthesize chiral MONs for chiral separation.

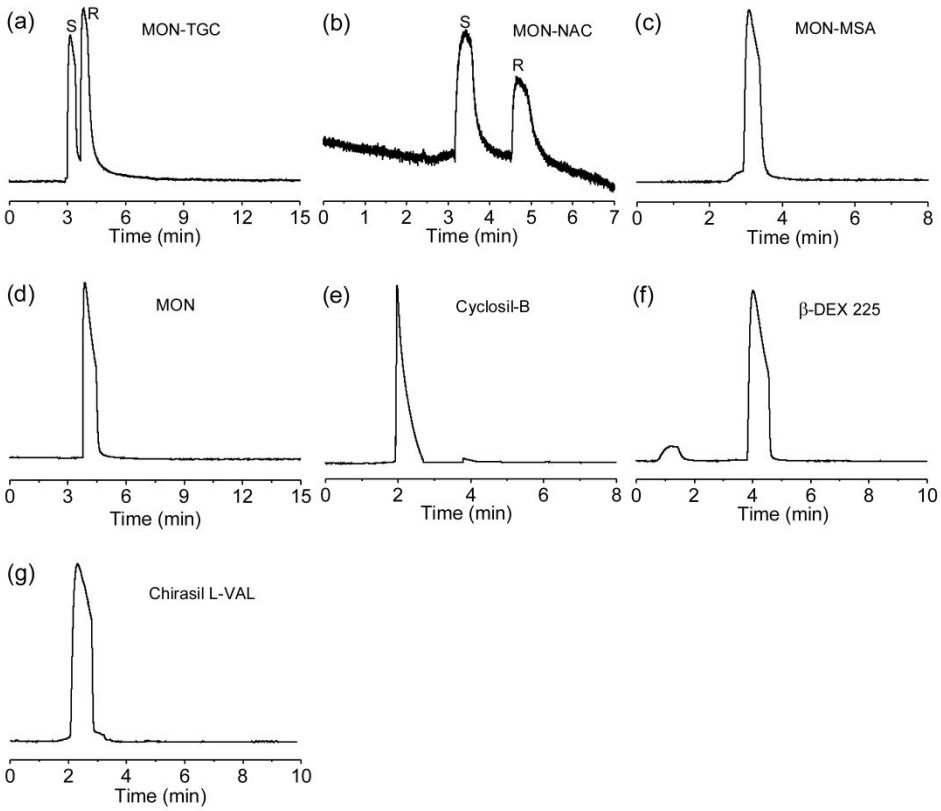

Figure 4. Gas chromatograms for the separation of 3-heptanol (140 °C) on: (a) MON-TGC; (b) MON-NAC; (c) MON-MSA; (d) MON; (e) Cyclosil-B; (f) β-DEX 225 and (g) Chirasil L-VAL. All the racemates were separated under the N_2 flow rate of 2 mL min^{-1}.

Table 1 The resolution (*R*s) and separation factor (*α*) for the separation of racemates on seven columns under the same separation conditions.

Racemates	Resolution (*R*s)[a]							Separation factor (α)[b]						
	T[c]	M[d]	N[e]	B[f]	225[g]	L[h]	O[i]	T	M	N	B	225	L	O
3-heptanol	1.31	-[j]	1.35	-	-	-	-	2.13	1.0	3.0	1.0	1.0	1.0	1.0
4-heptyn-2-ol	1.45	-	-	-	-	-	-	2.96	1.0	1.0	1.0	1.0	1.0	1.0
4-pentyn-2-ol	1.41	-	-	-	-	-	-	3.22	1.0	1.0	1.0	1.0	1.0	1.0
2-phenyl-4-penten-2-ol	1.68	-	-	-	-	-	-	3.56	1.0	1.0	1.0	1.0	1.0	1.0
methyl-2-chloropropionate	1.51	-	-	0.21	0.74	-	-	3.31	1.0	1.0	1.02	1.21	1.0	1.0
5-methyl-2-hexanol	1.64	-	-	-	-	-	-	3.80	1.0	1.0	1.0	1.0	1.0	1.0

[a] Calculated according to Rs = 2 (t_2-t_1) / (W_1 + W_2)

[b] Calculated according to α = t_2' / t_1'

[c] MON-TGC coated capillary column

[d] MON-MSA coated capillary column

[e] MON-NAC coated capillary column

[f] Cyclosil-B column

[g] β-DEX 225 column

[h] Chirasil L-VAL column

[i] MON coated capillary column

[j] cannot be separated

Although the chiral separation mechanisms are quite complicate and hard to illustrate, the chiral microenvironment of chiral MONs, π-π and hydrogen bonding interactions may have dominant roles in chiral separation. The pore size of three chiral MONs (> 11 Å) are larger than the kinetic diameters of the studied racemates (< 9.5 Å), suggesting that the chiral separation may occur in chiral MONs' pores (Figure 2b and Figure S9). To verify the significant characters of the chiral microenvironment of these chiral MONs, the pristine MON coated capillary column was compared (Figure S10). The studied racemates cannot be resolved on the pristine MON coated capillary column, revealing the microenvironment in these chiral MONs was essential for chiral separation. The hydrogen bonding sites from the -OH groups on TGC, -COOH groups on MSA as well as N-acetyl and -COOH groups on NAC were also crucial for the separation of chiral alcohols. In addition, the aromatic networks of chiral MONs' may provide π-π interaction for efficient separation of 4-heptyn-2-ol, 4-pentyn-2-ol, 2-phenyl-4-penten-2-ol, 4-hexyn-3-ol and 4-methyl-1-heptyn-3-ol with unsaturated double or triple bonds (Figure 3). However, the relatively strong π-π and hydrogen

bonding interaction of the racemates and chiral MONs may also lead to the tailing peaks of some racemates on these three chiral MONs coated columns.

Table 2. McReynolds Constants of Chiral MONs Coated Capillary Columns.

Column	X	Y	Z	U	S	Average
MON-TGC	113	275	204	225	247	212.8
MON-MSA	379	439	399	389	380	397.2
MON-NAC	417	658	492	614	449	526.0

The McReynolds constants of these chiral MONs coated capillary columns were further evaluated by using benzene (X, represented the weak dispersion forces and polarizability of the phase), n-butanol (Y, related to the hydrogen-bonding ability of the phase), 2-pentanone (Z, denoted to the polarizability and part of the dipolar character of the phase), nitropropane (U, related to the electron donor, electron acceptor and dipolar character of the phase), and pyridine (S, indicated the acidic character of the phase) as the probes (Table 2).[39] The average McReynolds constants ranged from 212.8 to 526.0, indicating the moderate to polar nature of the fabricated chiral MONs coated capillary

columns. These chiral MONs coated capillary columns all gave the largest Y values among five reference probes, proving the significant role of hydrogen-bonding ability of the fabricated chiral MONs coated capillary columns, which was favorable for the good separation of chiral alcohols. The entropy change (ΔS), enthalpy change (ΔH), the chiral part of entropy change ($\Delta\Delta S$) and enthalpy change ($\Delta\Delta H$) of the MON-TGC coated capillary column for *rac*-5-methyl-2-hexanol were further evaluated to study the chiral discrimination and retention of enantiomers (Figure S11 and Table S6). The obtained thermodynamic parameters were all negative, revealing that the chiral discrimination and retention of the studied enantiomers on MON-TGC coated capillary column were driven by enthalpy.[3,7]

To further show the advantage of these three chiral MONs coated capillary columns, three typical commercial chiral capillary columns (Cyclosil-B, β-DEX 225 and Chirasil L-VAL) were compared under the optimal conditions of individual columns (Figure S12-S14 and Table S3-S4). The MON-TGC coated capillary column gave better resolution and selectivity for the separation of 3-heptanol, 4-heptyn-2-ol, 4-pentyn-2-ol, 2-phenyl-4-penten-2-ol, and 5-methyl-2-hexanol as these chiral alcohols all could not be

separated on these three commercial columns. Similarly, MON-MSA coated capillary column showed higher resolution for 3-octanol, linalool and tetrahydrolinalool as these racemates all could not be separated on these three commercial columns. In addition, the MON-NAC coated capillary column offered better resolution for 3-heptanol, 4-methyl-1-heptyn-3-ol and 2-methyl-2,4-pentanediol than those on commercial columns. These results reveal the great potential of thiol-yne click strategy for post synthesis of chiral MONs in chiral separation.

4. CONCLUSIONS

In conclusions, we have reported the facile thiol-yne click strategy for rational design and post synthesis of three chiral MONs to fabricate their coated capillary columns for chiral GC. Depending on the difference of chiral molecules incorporated in the MON's networks, diverse racemates were well resolved and separated on their chiral MONs coated capillary columns. The chiral microenvironment, hydrogen bonding and π-π interactions of these chiral MONs played important roles in chiral GC. These chiral MONs coated capillary columns also provided superior selectivity and resolution for the studied chiral alcohols than three commercial columns. The present study has

developed a convenient and efficient approach to design and synthesize chiral MONs and also showed the first example of chiral MONs for chiral chromatography. This work will also largely facilitate the design, synthesis and application of chiral MONs in diverse domains. MONs with the merits of easy modification, tunable function and selectivity, and designable structures may receive increasing attention either in chemistry or in material science. In addition, the chiral MONs will possess great potential in chiral separation or catalysis. As the important roles of chiral drugs or biomolecules, the investigation of chiral MONs in the separation of chiral drugs or biomolecules should also be a significant direction.

ASSOCIATED CONTENT

Supporting Information

The Supporting Information is available free of charge on the ACS Publications website at DOI:

Additional information including instrumentation, and supplementary Figures and Tables (PDF).

AUTHOR INFORMATION

Corresponding Author

* E-mail: cxyang@nankai.edu.cn

ORCID

Yuan-Yuan Cui: 0000-0002-0874-7219

Cheng-Xiong Yang: 0000-0002-0817-2232

Xiu-Ping Yan: 0000-0001-9953-7681

Notes

There is no conflict to declare.

ACKNOWLEDGMENT

This work was supported by the National Natural Science Foundation of China (Nos. 21777074 and 21775056), the Tianjin Natural Science Foundation (No. 18JCQNJC05700), Tianjin Research Innovation Project of Postgraduate Students (2019YJSB082), Key Laboratory of Biological Resources of the Changbai Mountain & Functional Molecules (Yanbian University), Ministry of Education, and the Ph.D. Candidate Research Innovation Fund of the College of Chemistry Nankai University.

REFERENCES

(1) Zhang, M.; Chen, X. L.; Zhang, J. H.; Kong, J.; Yuan, L. M. A 3D Homochiral MOF $[Cd_2(d\text{-}cam)_3]\cdot 2Hdma\cdot 4dma$ for HPLC Chromatographic Enantioseparation. *Chirality* **2016**, *28*, 340-346.

(2) Liu, Y.; Xuan, W. M.; Cui, Y. Engineering Homochiral Metal-Organic Frameworks for Heterogeneous Asymmetric Catalysis and Enantioselective Separation. *Adv. Mater.* **2010**, *22*, 4112-4135.

(3) Kou, W. T.; Yang, C. X.; Yan, X. P. Post-Synthetic Modification of Metal-Organic Frameworks for Chiral Gas Chromatography. *J. Mater. Chem. A* **2018**, *6*, 17861-17866.

(4) Xie, S. M.; Zhang, Z. J.; Wang, Z. Y.; Yuan, L. M. Chiral Metal-Organic Frameworks for High-Resolution Gas Chromatographic Separations. *J. Am. Chem. Soc.* **2011**, *133*, 11892-11895.

(5) Zhang, S. N.; Zheng, Y. L.; An, H. D.; Aguila, B.; Yang, C. X.; Dong, Y. Y.; Xie, W.; Cheng, P.; Zhang, Z. J.; Chen, Y.; Ma, S. Q. Covalent Organic Frameworks with Chirality Enriched by Biomolecules for Efficient Chiral Separation. *Angew. Chem. Int. Ed.* **2018**, *57*, 16754-16759.

(6) Han, X.; Huang, J. J.; Yuan, C.; Liu, Y.; Cui, Y. Chiral 3D Covalent Organic Frameworks for High Performance Liquid Chromatographic Enantioseparation. *J. Am. Chem. Soc.* **2018**, *140*, 892-895.

(7) Qian, H. L.; Yang, C. X.; Yan, X. P. Bottom-up Synthesis of Chiral Covalent Organic Frameworks and Their Bound Capillaries for Chiral Separation. *Nat. Commun.* **2016**, *7*, 12104.

(8) Malik, A. U.; Gan, F. W.; Shen, C. S.; Yu, N.; Wang, R. B.; Crassous, J.; Shu, M. H.; Qiu, H. B. Chiral Organic Cages with a Triple-Stranded Helical Structure Derived from Helicene. *J. Am. Chem. Soc.* **2018**, *140*, 2769-2772.

(9) Chen, L. J.; Reiss, P. S.; Chong, S. Y.; Holden, D.; Jelfs, K. E.; Hasell, T.; Little, M. A.; Kewley, A.; Briggs, M. E.; Stephenson, A.; Thomas, K. M.; Armstrong, J. A.; Bell, J.; Busto, J.; Noel, R.; Liu, J.; Strachan, D. M.; Thallapally, P. K.; Cooper, A. I. Separation of Rare Gases and Chiral Molecules by Selective Binding in Porous Organic Cages. *Nat. Mater.* **2014**, *13*, 954-960.

(10) Xie, S. M.; Fu, N.; Li, L.; Yuan, B. Y.; Zhang, J. H.; Li, Y. X.; Yuan, L. M. Homochiral Metal-Organic Cage for Gas Chromatographic Separations. *Anal. Chem.* **2018**, *90*, 9182-9188.

(11) Chun, J.; Park, J. H.; Kim, J.; Lee, S. M.; Kim, H. J.; Son, S. U. Tubular-Shape Evolution of Microporous Organic Networks. *Chem. Mater.* **2012**, *24*, 3458-3463.

(12) Kang, N.; Park, J. H.; Jin, M. S.; Park, N.; Lee, S. M.; Kim, H. J.; Kim, J. M.; Son, S. U. Microporous Organic Network Hollow Spheres: Useful Templates for Nanoparticulate Co_3O_4 Hollow Oxidation Catalysts. *J. Am. Chem. Soc.* **2013**, *135*, 19115-19118.

(13) Yoo, J.; Park, N.; Park, J. H.; Park, J. H.; Kang, S.; Lee, S. M.; Kim, H. J.; Jo, H.; Park, J.-G.; Son, S. U. Magnetically Separable Microporous Fe-Porphyrin Networks for Catalytic Carbene Insertion into N-H Bonds. *ACS Catal.* **2015**, *5*, 350-355.

(14) Ma, L.; Liu, Y. L.; Liu, Y.; Jiang, S. Y.; Li, P.; Hao, Y. C.; Shao, P. P.; Yin, A. X.; Feng, X.; Wang, B. Ferrocene-Linkage-Facilitated Charge Separation in Conjugated Microporous Polymers. *Angew. Chem. Int. Ed.* **2019**, *58*, 4221-4226.

(15) Li, X.; Li, Z.; Yang, Y. W. Tetraphenylethylene-Interweaving Conjugated Macrocycle Polymer Materials as Two-Photon Fluorescence Sensors for Metal Ions and Organic Molecules. *Adv. Mater.* **2018**, *30*, 1800177.

(16) Park, N.; Ko, K. C.; Shin, H.-W.; Lee, S. M.; Kim, H. J.; Lee, J. Y.; Son, S. U. Tandem Generation of Isocoumarins in Hollow Microporous Organic Networks: Nitrophenol Sensing Based on Visible Light. *J. Mater. Chem. A* **2016**, *4*, 8010-8014.

(17) Xu, M. Y.; Wang, T.; Gao, P.; Zhao, L.; Zhou, L.; Hua, D. B. Highly Fluorescent Conjugated Microporous Polymers for Concurrent Adsorption and Detection of Uranium. *J. Mater. Chem. A* **2019**, *7*, 11214-11222.

(18) Jia, Y. Q.; Su, H.; Wang, Z. H.; Wong, Y.-L. E.; Chen, X. F.; Wang, M. L.; Chan, T.-W. D. Metal-Organic Framework@Microporous Organic Network as Adsorbent for Solid-Phase Microextraction. *Anal. Chem.* **2016**, *88*, 9364-9367.

(19) Hong, S.; Yoo, J.; Park, N.; Lee, S. M.; Park, J.-G.; Park, J. H.; Son, S. U. Hollow Co@C Prepared from a Co-ZIF@Microporous Organic Network: Magnetic Adsorbents for Aromatic Pollutants in Water. *Chem. Commun.* **2015**, *51*, 17724-17727.

(20) Zhang, C.; Qiao, Y.; Xiong, P. X.; Ma, W. Y.; Bai, P. X.; Wang, X.; Li, Q.; Zhao, J.; Xu, Y. F.; Chen, Y.; Zeng, J. H.; Wang, F.; Xu, Y. H.; Jiang, J. X. *ACS Nano* **2019**, *13*, 745-754.

(21) Molina, A.; Patil, N.; Ventosa, E.; Liras, M.; Palma, J.; Marcilla, R. New Anthraquinone-Based Conjugated Microporous Polymer Cathode with Ultrahigh Specific Surface Area for High-Performance Lithium-Ion Batteries. *Adv. Funct. Mater.* **2019**, 1908074.

(22) Kang, C. W.; Choi, J.; Ko, Y.-J.; Lee, S. M.; Kim, H. J.; Kim, H. J.; Kim, J. P.; Son, S. U. Thin Coating of Microporous Organic Network Makes a Big Difference: Sustainability Issue of Ni Electrodes on the PET Textile for Flexible Lithium-Ion Batteries. *ACS Appl. Mater. Interfaces* **2017**, *9*, 36936-36943.

(23) Jang, J. Y.; Le, T. M. D.; Ko, J. H.; Ko, Y.-J.; Lee, S. M.; Kim, H. J.; Jeong, J. H.; Thambi, T.; Lee, D. S.; Son, S. U. Triple-, Double-, and Single-Shelled Hollow Spheres of Sulfonated Microporous Organic Network as Drug Delivery Materials. *Chem. Mater.* **2019**, *31*, 300-304.

(24) Jang, J. Y.; Duong, H. T. T.; Lee, S. M.; Kim, H. J.; Ko, Y.-J.; Jeong, J. H.; Lee, D. S.; Thambi, T.; Son, S. U. Folate Decorated Hollow Spheres of Microporous Organic Networks as Drug Delivery Materials. *Chem. Commun.* **2018**, *54*, 3652-3655.

(25) Liang, B.; Wang, H.; Shi, X. H.; Shen, B. Y.; He, X.; Ghazi, Z. A.; Khan, N. A.; Sin, H.; Khattak, A. M.; Li, L. S.; Tang, Z. Y. Microporous Membranes Comprising Conjugated Polymers with Rigid Backbones Enable Ultrafast Organic-Solvent Nanofiltration. *Nat. Chem.* **2018**, *10*, 961-967.

(26) Wang, X.; Li, J.; Lu, S. M.; Liu, Y.; Li, C. Efficient Enantioselective Hydrogenation of Quinolines Catalyzed by Conjugated Microporous Polymers with Embedded Chiral BINAP Ligand. *Chin. J. Catal.* **2015**, *36*, 1170-1174.

(27) Wei, J.; Zhang, X. M.; Zhao, Y. P.; Li, R. X. Chiral Conjugated Microporous Polymers as Novel Chiral Fluorescence Sensors for Amino Alcohols. *Macromol. Chem. Phys.* **2013**, *214*, 2232-2238.

(28) Wang, X. R.; Zhang, J.; Liu, Y.; Cui, Y. Chiral Porous TADDOL-Embedded Organic Polymers for Asymmetric Diethylzinc Addition to Aldehydes. *Bull. Chem. Soc. Jpn.* **2014**, *87*, 435-440.

(29) Ratvijitvech, T.; Dawson, R.; Laybourn, A.; Khimyak, Y. Z.; Adams, D. J.; Cooper, A. I. Post-Synthetic Modification of Conjugated Microporous Polymers. *Polymer* **2014**, *55*, 321-325.

(30) Lowe, A. B.; Hoyle, C. E.; Bowman, C. N. Thiol-Yne Click Chemistry: A Powerful and Versatile Methodology for Materials Synthesis. *J. Mater. Chem.* **2010**, *20*, 4745-4750.

(31) Kiskan, B.; Weber, J. Versatile Postmodification of Conjugated Microporous Polymers Using Thiol-Yne Chemistry. *ACS Macro Lett.* **2012**, *1*, 37-40.

(32) Kang, C. W.; Ko, Y.-J.; Lee, S. M.; Kim, H. J.; Son, S. U. Poly(ethylene terephthalate) Fibers with a Thin Layer of Click-Based Microporous Organic Network: Enhanced Capture Performance toward $PM_{2.5}$. *Adv. Mater. Interfaces* **2018**, *5*, 1800628.

(33) Wang, X. P.; Zhao, X. D.; Dong, W. B.; Zhang, X. H.; Xiang, Y. G.; Huang, Q. Y.; Chen, H. Integrating Amino Groups within Conjugated Microporous Polymers by Versatile Thiol-Yne Coupling for Light-Driven Hydrogen Evolution. *J. Mater. Chem. A* **2019**, *7*, 16277-16284.

(34) Han, X. L.; Xu, M. Y.; Yang, S.; Qian, J.; Hua, D. B. Acetylcysteine-Functionalized Microporous Conjugated Polymers for Potential Separation of Uranium from Radioactive Effluents. *J. Mater. Chem. A* **2017**, *5*, 5123-5128.

(35) Ko, J. H.; Lee, S. M.; Kim, H. J.; Ko, Y.-J.; Son, S. U. Skeleton Carbonylation of Conjugated Microporous Polymers by Osmium Catalysis for Amine-Rich Functionalization. *ACS Macro Lett.* **2018**, *7*, 1353-1358.

(36) Jiang, J. X.; Su, F. B.; Trewin, A.; Wood, C. D.; Campbell, N. L.; Niu, H. J.; Dickinson, C.; Ganin, A. Y.; Rosseinsky, M. J.; Khimyak, Y. Z.; Cooper, A. I. Conjugated Microporous Poly(aryleneethynylene) Networks. *Angew. Chem. Int. Ed.* **2007**, *46*, 8574-8578.

(37) Cui, Y. Y.; Ren, H. B.; Yang, C. X.; Yan, X. P. Room-Temperature Synthesis of Microporous Organic Network for Efficient Adsorption and Removal of Tetrabromobisphenol A from Aqueous Solution. *Chem. Eng. J.* **2019**, *368*, 589-597.

(38) Kewley, A.; Stephenson, A.; Chen, L. J.; Briggs, M. E.; Hasell, T.; Cooper, A. I. Porous Organic Cages for Gas Chromatography Separations. *Chem. Mater.* **2015**, *27*, 3207-3210.

(39) Berthod, A. Determination and Use of Rohrschneider-McReynolds Constants for Chiral Stationary Phases Used in Capillary Gas Chromatography. *Anal. Chem.* **1995**, *67*, 849-857.

For Table of Contents Only